

Research Article

Study of Materials for Drugs Delivery: *cis*-[PtCl₂(NH₃)₂] Hydrolysis on Functionalized SiO₂(100) Surfaces

A. Díaz Compañy,¹ G. Brizuela,¹ and S. Simonetti^{1,2}

¹ Universidad Nacional del Sur, IFISUR, CONICET, Avenida Alem 1253, 8000 Bahía Blanca, Argentina

² Universidad Tecnológica Nacional, 11 de Abril 461, 8000 Bahía Blanca, Argentina

Correspondence should be addressed to S. Simonetti; ssimonet@uns.edu.ar

Received 17 August 2013; Revised 27 October 2013; Accepted 19 November 2013

Academic Editor: Shi J. Xu

Copyright © 2013 A. Díaz Compañy et al. This is an open access article distributed under the Creative Commons Attribution License, which permits unrestricted use, distribution, and reproduction in any medium, provided the original work is properly cited.

The hydrolysis of the *cis*-platin drug on a SiO₂(100) hydrated surface was investigated by computational modeling. The *cis*platin molecule presents weak interactions with the neighbouring OH groups of the hydrated surface. The *cis*platin hydrolysis is not favourable on the SiO₂(100) surface. Consequently, the adsorption properties of SiO₂(100) are improved considering the surface's modification with K, Mg, or NH₂ functional species. In general, the system is more stable and the molecule-surface distance is reduced when *cis*platin is adsorbed on the promoted surfaces. The hydrolysis is a favourable process on the SiO₂(100) functionalized surfaces. The *cis*platin hydrolysis is most favoured when the surface is functionalized with the NH₂ specie. The electron density exchange plays a main role in the adsorption process. *cis*-[PtCl₂(NH₃)₂] and *cis*-[PtCl(NH₃)₂]⁺ are adsorbed on the functionalized surface via Cl-N and Cl-Si interactions, while the *cis*-[Pt(NH₃)₂]²⁺ complex is adsorbed through Pt-O, Pt-Si, and Pt-H interactions. After adsorption, the strength of the N-Si, Si-O, and N-H superficial bonds of the functionalized SiO₂(100) changes favouring the interaction between the molecule and their complexes with the surface.

1. Introduction

Silica (SiO₂) is a very important material in both industrial application and material science. Various problems related to silica surface characteristics are encountered in different areas of science and technology: physics, chemistry and physical chemistry, agriculture, soil science, biology and medicine, electrical energetic, the oil processing industry, the metallurgical and mining industries, some fields of geology, and so forth. In the past, many reviews and significant articles have appeared on the subject of surface chemistry of silica [1–10].

Different types of silica are widely used as efficient adsorbents, selective absorbents, and active phase carriers in catalysis. Chemical modification of the surface of silica receives interest because this process allows researchers to regulate and change adsorption properties and technological characteristics; for example, the alkylation techniques have

served as the starting point for bonding more interesting and complicated molecules to the surface [11] such as polymers [12], saccharides [13], and amines [14, 15]. At the crystal surface, Si atoms are no longer protected by the bulk material from chemical reactions with the environment, and molecular species can be absorbed into or bond with surface atoms. These new molecular species can alter the electronic structure and bonding of the SiO₂ at the surface.

Studies have shown that silica matrixes could improve drug delivery systems [16, 17]. Our group have previously studied the adsorption of *cis*-platin on a SiO₂(111) surface. *cis*-platin (*cis*-[PtCl₂(NH₃)₂]) is a coordination compound, used in the treatment of several solid tumors [18, 19]. *cis*-platin and its hydrolysis products (*cis*-[PtCl(NH₃)₂]⁺ and *cis*-[Pt(NH₃)₂]²⁺) exhibit a grand pharmacological effect [20–24], but they have adverse secondary effects [25, 26]. However, the optimization of the dosing and delivery schedule can possibility minimise unfavourable effects while maintaining

effectiveness [27, 28]. We have studied the adsorption of *cis*-platin and its complexes on a $\text{SiO}_2(111)$ hydrated surface by tight binding calculation [29]. We have reproduced the main characteristics of the adsorption process showing a possible way for the molecule/complexes adsorption. We have also analyzed the nature of the drug-carrier bonding and the changes observed in the electronic structure upon adsorption. Except those molecular orbitals lying much lower in energy, the rest are modified showing the molecule-surface interaction. The new interactions are formed at expenses of the OH bonds. One of the major findings is the Cl-H interaction that takes place during *cis*- $[\text{PtCl}_2(\text{NH}_3)_2]$ and *cis*- $[\text{PtCl}(\text{NH}_3)_2]^+$ adsorptions and the Pt-O interaction developed during the *cis*- $[\text{Pt}(\text{NH}_3)_2]^{2+}$ adsorption. The adsorption of *cis*-platin on a SH functionalized $\text{SiO}_2(111)$ surface has also been studied [30]. The molecule/complexes-SH electrondonating effect plays an important role in the catalytic reaction. The more important drug-carrier interactions occur through the Cl-H, Pt-S, and Pt-H interactions. When the new interactions are formed, the functionalized carrier maintains its matrix properties while the molecule is the most affected after adsorption. The Pt atomic orbitals present the most important changes during adsorption. We have also evaluated the adsorption effects of CN-functionalized $\text{SiO}_2(111)$ surface as *cis*-platin drug's host [31]. The CN-silica carrier showed good catalytic properties. The molecule-surface interactions are strengthening due to the incorporation of the CN silane group. The remarkable properties of the functionalized carrier may be attributed to the smaller changes in the CN groups caused by the interaction with neighbouring *cis*-platin molecules and the enhancement in Pt-bonding interactions due to the surface incorporation of CN silane groups.

In the present study, we analyze the adsorption of *cis*-platin and its products on a dominant surface of the hydrated silica, a $\text{SiO}_2(100)$ plane, and the surface functionalization with K, Mg, CH_3 , or NH_2 chemical species in order to improve the catalytic process. The minimum energy geometry of *cis*-platin and its complexes is calculated, and the changes in the electronic structure and the chemical bonding are addressed by Yet Another Extended Hückel Molecular Orbital Package (YAEHMOP) [32].

2. The Drug-Carrier System

It is known that hydroxyl (silanol) groups, Si-OH , should be present on the surface of silicates and silicas. We have simulated completely hydrated silica by considering it comparable to the (100) surface of β -cristobalite, in which each surface Si atom is connected to a single silanol group [33]. The crystal structure of β -cristobalite is based on networks of corner-connected SiO_4 tetrahedra, with noncollinear Si-O-Si bonds forming bond angles of approximately 147° . Si superficial atoms tend to have a complete tetrahedral configuration and, in an aqueous medium, their free bonds become saturated with hydroxyl groups forming silanol groups ($=\text{Si-OH}$).

We have used a supercell of 469 atoms: 113 Si, 274 O atoms, and 82 H atoms, distributed in six layers. Every Si atom completes its tetrahedron with O atoms. As a starting

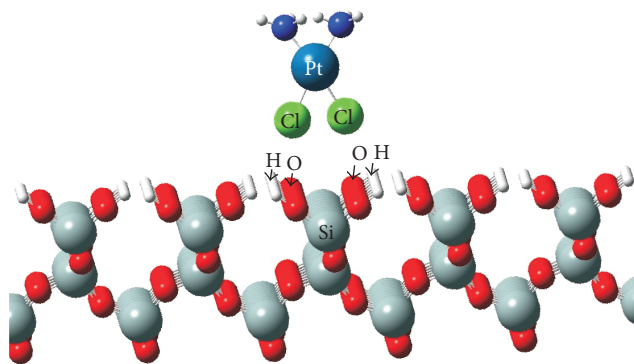


FIGURE 1: Schematic lateral view of the *cis*-platin adsorption geometry on the $\text{SiO}_2(100)$ hydrated surface.

geometry for the surface, we used the following distances: Si-Si, 5.07 Å; Si-O (surface), 1.5 Å; O-O (bulk), 2.53 Å; O-H, 0.96 Å, and H-H, 5.07 Å. In order to reproduce the surface, this cell is extended in two dimensions parallel to the surface. All dangling bonds were saturated with additional H atoms. On the other hand, the starting point for the calculation was the *cis*-platin structure (see Figure 1) taken from experimental data [34, 35]. Initial optimization of *cis*-platin agreed with the findings of several theoretical studies [36] giving a C_{2v} minimum with a distorted square-planar coordination. The in-plane N-H groups are aligned toward Cl, resulting in (N-H)---Cl distances and angles of 2.41 Å and 113° . The electrostatic potential shows a highly polar molecule more positive on the amino group and negative on the chlorine atoms. The Pt is close to neutral.

3. The Computational Method

Our calculations were performed using the Atom Superposition and Electron Delocalization method [37–39]. This method is a modification of the Extended Hückel Molecular Orbital Method implemented with the YAEHMOP program (Yet Another Extended Hückel Molecular Orbital Package) [32]. The Extended Hückel (EH) based methods supply useful information about different aspects of the electronic structure and the chemical reactivity. The theory is based on a physical model of molecular and solid electronic charge density distribution functions [40, 41]. The EH method has been successfully employed for experimental information analysis and its correlation with atomic data. It is a methodology that reveals the basic interactions that are responsible for the chemical bonding and it makes possible the relationship between systems with similar geometrical and compositional distributions. An other advantage of the method is that it allows working with systems that include hundred transition metals per unit cell. The literature shows a lot of references about the application of this method in catalysis and adsorption phenomena on surfaces [42–45]. Our group has recently used this methodology in studies of industrial interest [46, 47].

We have computed the adiabatic energy of the system absorbing the drug *cis*-platin on the $\text{SiO}_2(100)$ hydrated

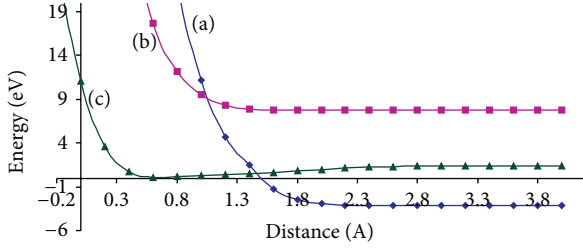


FIGURE 2: Adiabatic total energy curves for the (a) *cis*-platin-silica system, (b) *cis*-[PtCl(NH₃)₂]⁺-silica system, and (c) *cis*-[Pt(NH₃)₂]²⁺-silica system.

surface (carrier). During the calculations, the structures of both molecule and substrate were optimized at steps of 0.02 Å and convergence in energy of 0.01 eV. We have obtained the energy curves, initially for the *cis*-platin molecule and then considered the removal of one and the two chloroatoms of the molecule, in order to study the hydrolysis phenomenon. In a second stage, we have modified the SiO₂(100) surface by adding a functional specie (K, Mg, CH₃, or NH₂), in order to analyze the changes in the surface adsorption properties.

The adiabatic total energy values were computed as the difference between the electronic energy (E) of the system when the drug is at finite distance on the surface (carrier) and the same energy when that drug is far away from the surface:

$$\Delta E_{\text{Abs, total}} = E(\text{carrier} + \text{drug}) - E(\text{carrier}) - E(\text{drug}). \quad (1)$$

To understand the drug-carrier interactions we used the concept of density of states (DOS) and crystal orbital overlap population (COOP) curves. The DOS curve is a plot of the number of orbitals per unit volume per unit energy. The COOP curve is a plot of the overlap population weighted DOS versus energy. The integration of the COOP curve up to the Fermi level (E_f) gives the total overlap population of the bond specified and it is a measure of the bond strength.

4. Results and Discussion

The adsorption energies for *cis*-platin and its complexes are shown in Figure 2. The *cis*-[PtCl₂(NH₃)₂] molecule adopt its minimum energy location at the OH-Cl distance of 2.4 Å. When we computed the *cis*-platin complexes adsorption energies, the [PtCl(NH₃)₂]⁺ and *cis*-[Pt(NH₃)₂]²⁺ adsorptions are not favourable because the energy is always positive (repulsive interaction). We can conclude that the hydrolysis process is not favourable on the SiO₂(100) hydrated surface. For *cis*-[PtCl₂(NH₃)₂]-silica configuration of minimum energy, each Cl atom of *cis*-platin presents weak interactions with neighbour OH groups of the hydrated surface. The existence of these bonds is confirmed by the bond population; the Cl-H and Cl-O overlap populations (OP) are 0.011 and 0.013, respectively. The COOP curves can be seen in Figures 3(a) and 3(b). These curves present bonding and antibonding peaks below the Fermi Energy level (E_f) and their integration up to the E_f gives the cited small total OPs. After adsorption,

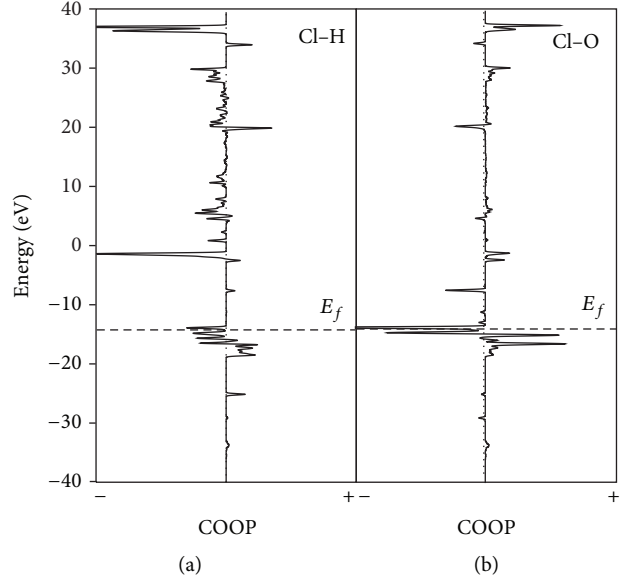


FIGURE 3: COOP curves for the (a) Cl-H interactions and (b) Cl-O interactions in the *cis*-platin-silica system.

TABLE 1: Average overlap population (OP).

Bond	OP
Cl-H	0.011 ^a
Cl-O	0.013 ^a
Cl-Pt	0.418 ^a 0.418 ^b
O-H	0.600 ^a 0.607 ^b
O-Si	0.591 ^a 0.593 ^b

^a *cis*-[PtCl₂(NH₃)₂]/silica system.

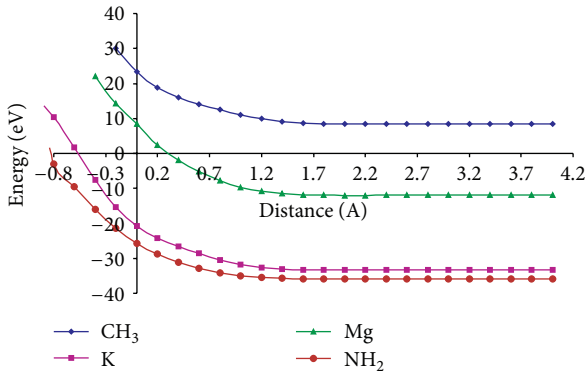
^b Bare silica or isolated *cis*platin.

the silica surface almost maintains its matrix properties. The O-H and O-Si superficial bonds only decrease 1.21% and 0.38%, respectively (see Table 1); the orbital population changes are smaller than 2%. The major changes occur in *cis*-platin's molecule; the Cl-Pt OP decreases 22%. The Cl *s* and Cl *p* populations decrease 5% and 47%, respectively, while the Pt *s*, Pt *p*, and Pt *d* orbital populations change 37%, 35%, and 90%, respectively. A complete data about the orbital populations and net charges can be seen in Table 2.

In a second stage, in order to improve the adsorption properties of the SiO₂(100) surface, we have considered the surface's modification with different functional species: K, Mg, CH₃, or NH₂. Figure 4 shows the energy curves for these systems. When the surface is functionalized by CH₃, the adsorption process is not favourable (the energy of this system is always positive) and it could occur because the interaction between the CH₃ functional group and *cis*-platin molecule is not favoured by the electron exchange; while the other systems (promoted by K, Mg, or NH₂) are more stable than the surface without functionalization, in general

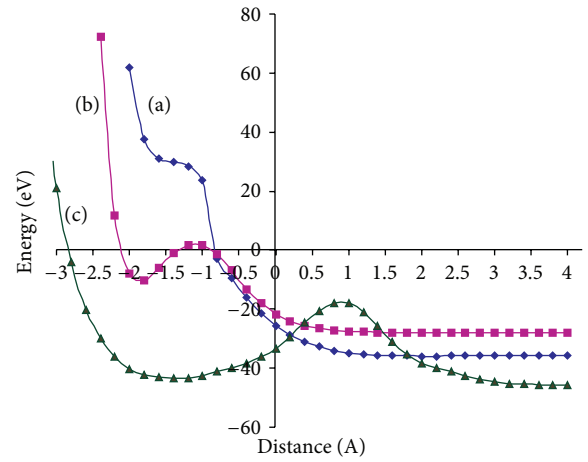
TABLE 2: Orbital occupations and net charge.

Atom	s	p_x	p_y	p_z	$d_{x^2-y^2}$	d_{z^2}	d_{xy}	d_{xz}	d_{yz}	Charge
Cl	1.7768 ^a	0.9422 ^a	0.9907 ^a	1.0210 ^a						+2.2692 ^a
	1.8612 ^b	1.7473 ^b	1.9174 ^b	1.8722 ^b						-0.3982 ^b
Pt	0.4043 ^a	0.2285 ^a	0.1692 ^a	0.1824 ^a	0.0693 ^a	0.0698 ^a	0.2711 ^a	0.3358 ^a	0.0937 ^a	+8.1759 ^a
	0.6591 ^b	0.3367 ^b	0.2133 ^b	0.3421 ^b	1.8970 ^b	1.9930 ^b	1.6842 ^b	1.0725 ^b	1.9481 ^b	-0.1459 ^b
H	0.5729 ^a									+0.4271 ^a
	0.5770 ^b									+0.4230 ^b
O	1.6225 ^a	1.6688 ^a	1.7906 ^a	1.7730 ^a						-0.8548 ^a
	1.6203 ^b	1.7708 ^b	1.7888 ^b	1.7728 ^b						-0.9527 ^b
Si	0.5596 ^a	0.3472 ^a	0.3426 ^a	0.3458 ^a						+2.3648 ^a
	0.5994 ^b	0.3488 ^b	0.3432 ^b	0.3469 ^b						+2.3617 ^b

^a *cis*-[PtCl₂(NH₃)₂]/silica system.^b Bare silica or isolated *cis*platin.FIGURE 4: Adiabatic total energy curves for the *cis*-platin adsorption on silica functionalized with Mg, K, CH₃, and NH₂ chemical species.

the surface modification acts on reducing the adsorption energy. The curves corresponding to the systems promoted by K, Mg, and NH₂ do not present an absolute minimum energy position for the *cis*-platin molecule. In general, the more favorable molecule-surface distances are in the range between 0.3 and 4.0 Å. We can conclude that the surface functionalization improves the adsorbate-substrate contact by diminishing the molecule-surface distance and reducing the adsorption energy.

The system functionalized with NH₂ group presents the best *cis*-platin adsorption energies compared to the other studied systems (see Figure 4). We have calculated the adsorption of *cis*-platin and its products, [PtCl(NH₃)₂]⁺ and *cis*-[Pt(NH₃)₂]²⁺, on the silica-NH₂ matrix; Figure 5 shows the corresponding adiabatic curves. We can observe that *cis*-platin and [PtCl(NH₃)₂]⁺ adsorptions are favourable on the surface (at positive distances), while [Pt(NH₃)₂]²⁺ adsorption is more stable inside the surface (at negative distances). A schematic view of the adsorption geometry can be seen in Figure 6 (see selected $h = 0$ level). We can see in Figure 5 that the adsorption of [Pt(NH₃)₂]²⁺ complex on the silica-NH₂ matrix is the most favoured; the minimum adsorption energy is obtained when the complex is located at -1.4 Å from the surface. In order to analyze the complexes-surface

FIGURE 5: Adiabatic total energy curves for the (a) *cis*-platin-silica-NH₂ system, (b) *cis*-[PtCl(NH₃)₂]⁺-silica-NH₂ system, and (c) *cis*-[Pt(NH₃)₂]²⁺-silica-NH₂ system.

interactions, we have studied in detail the electronic structure and bonding characteristics of the *cis*-platin/SiO₂(100)-NH₂ system.

The DOS curve corresponding to the isolated SiO₂(100)-NH₂ system can be seen in Figure 7(a). When the molecule is adsorbed, the changes are lightly perceived (see Figure 7(b)). For a major view of these states, the partial DOS of the *cis*-platin, arranged in the same geometry as the molecules take on the surface, is shown in Figure 7(c). The horizontal sticks display the energy of the molecular orbitals in the isolated *cis*-platin molecule. After adsorption, a portion of its DOS is pushed above the Fermi level. The Fermi level is modified and this implies an energetic stabilization of the molecule after adsorption. The lowest *s* and *p* orbitals of the molecule substantially interact with surface *s-p* orbitals; the corresponding bands are spread out after adsorption.

For *cis*-[PtCl₂(NH₃)₂]-silica-NH₂ study, we have selected the complex located at 2.0 Å from the surface. For this configuration, the Cl atoms present interactions with neighbouring N and Si atoms of the surface. The Cl-N and Cl-Si overlap populations are 0.8105 and 0.5785, respectively;

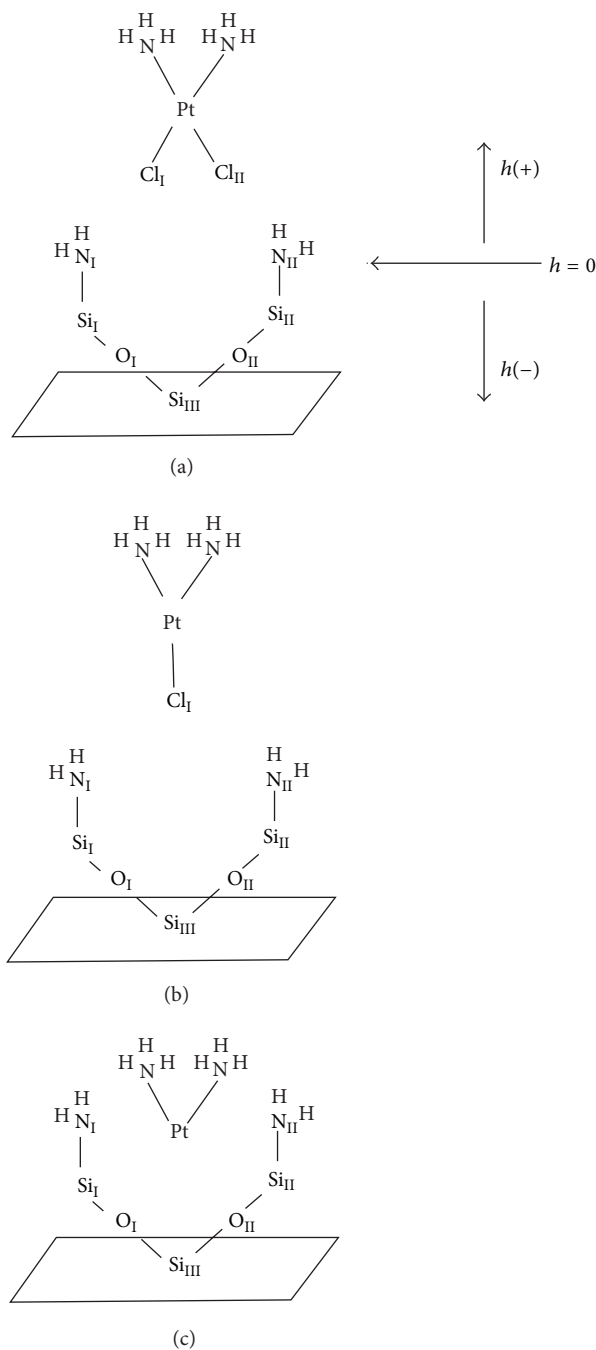


FIGURE 6: The schematic drawing of the adsorption geometries is indicated in (a) *cis*-platin/ NH_2 -silica system, (b) *cis*- $[\text{PtCl}(\text{NH}_3)_2]^+$ / NH_2 -silica system, and (c) *cis*- $[\text{Pt}(\text{NH}_3)_2]^{2+}$ / NH_2 -silica system.

the COOP curves can be seen in Figures 8(a) and 8(b). No other important interactions were observed. For *cis*- $[\text{PtCl}(\text{NH}_3)_2]^+$ -silica- NH_2 system we have considered for studying the geometry corresponding to the complex positioned at 2.0 \AA from the surface (at its minimum energy location). When the *cis*-platin molecule loses the first chloro atom, the most favourable interactions take place between the remaining Cl atom and the neighbouring N and Si atoms of the surface. The Cl-N and Cl-Si OP values are 0.7402 and 0.4235 respectively; Figures 8(c) and 8(d) show the

corresponding COOPs curves. For *cis*- $[\text{PtCl}(\text{NH}_3)_2]^+$ -silica- NH_2 system, we have selected for studying the geometry corresponding to the complex positioned at -1.4 \AA from the surface (at its minimum energy location). When the molecule loses both the chloro atoms, the most favourable interactions occur between the Pt atom and neighbouring O and Si atoms of the surface. The Pt-O OP value is 0.7269, while the Pt-Si OP values are 0.1092 (Si superficial) and 0.0285 (Si bulk). A very small Pt-H interaction is detected (OP = 0.002). Figure 9 shows the corresponding COOPs curves.

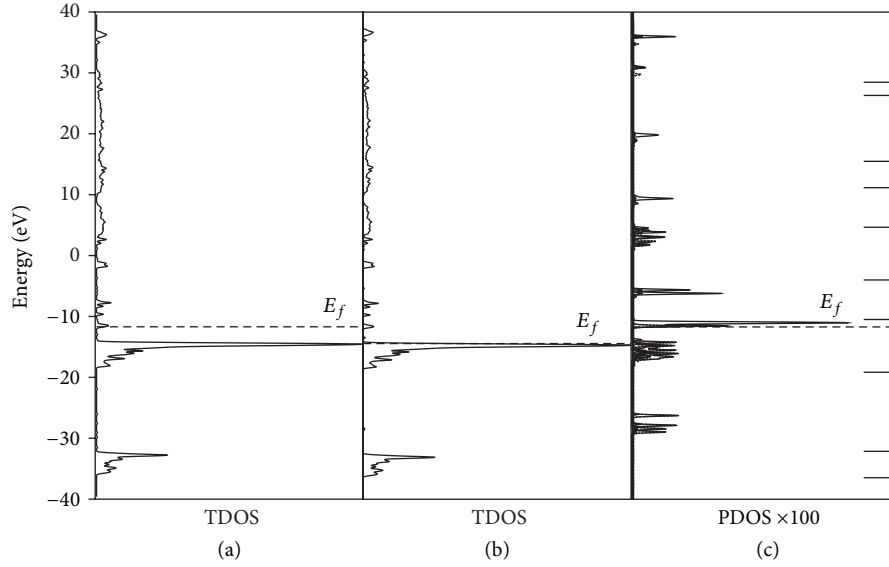


FIGURE 7: (a) Total DOS for the *cis*-platin-silica/ NH_2 system, (b) total DOS for the isolated silica/ NH_2 system, and (c) projected DOS for the *cis*-platin molecule adsorbed on the silica surface. The horizontal solid lines indicate the orbital positions in the isolated *cis*-platin molecule.

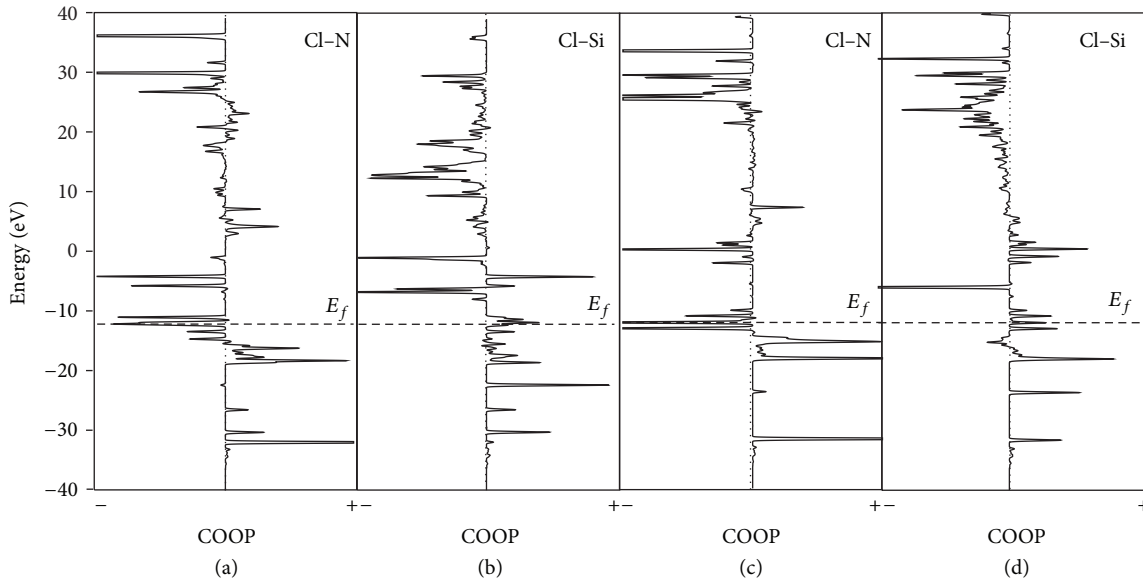


FIGURE 8: COOP curves for the Cl-N and Cl-Si interactions—(a) and (b) for *cis*- $[\text{PtCl}_2(\text{NH}_3)_2]$ adsorption and (c) and (d) for *cis*- $[\text{PtCl}(\text{NH}_3)_2]^+$ adsorption.

During adsorption, an electronic densities relocation is produced between the surface and *cis*-platin atomic orbitals. The major changes are summarized in Table 3. For *cis*- $[\text{PtCl}_2(\text{NH}_3)_2]$ -silica- NH_2 system, the *s* and *p* orbital populations of the N atoms neighbouring to *cis*-platin decrease 1–7% and increase 39–46%, respectively. The *s* and *p* populations of neighbouring Si (superficial) atoms decrease 9–11% and increase 2–9% respectively, while Si (bulk) atom population decreases less than 1%. The *s* and *p* orbital populations of the O atoms neighbouring to *cis*-platin increase to about 1% and 4–13%, respectively. Then, the major population changes occur in N *p*, Si (superficial) *s*, and O *p* orbitals. The

biggest percent changes in the *cis*-platin orbital populations are observed. The Cl *s* and Cl *p* populations decrease 15–22%, and 40–51% respectively, while Pt *s*, Pt *p*, and Pt *d* populations decrease 38%, 31%, and 77%, respectively. For *cis*- $[\text{PtCl}(\text{NH}_3)_2]^+$ -silica- NH_2 system, the *s* and *p* orbital populations of the N atoms neighbouring to *cis*-platin modified 1–8% and 59–87%, respectively. The *s* and *p* populations of neighbouring Si(superficial) atoms are modified 1–9% and increase 4–6%, respectively, while Si (bulk) population decreases less than 1%. The *s* and *p* orbital populations of the O atoms neighbouring to *cis*-platin increase to about 1% and 3–14%, respectively. Then, the major population

TABLE 3: Orbital occupations, net charges, and average overlap population (OP).

	Orbital occupation			Charge	Bond	OP
	<i>s</i>	<i>p</i>	<i>d</i>			
Cl _I	1.4606 ^a	2.6716 ^a		2.8678 ^a	Cl-N	0.8105 ^a
	1.5438 ^b	3.6228 ^b		1.8333 ^b		0.7402 ^b
	—	—		—		—
	1.8613 ^d	5.5367 ^d		-0.3980 ^d		—
Cl _{II}	1.5858 ^a	3.3345 ^a		2.0796 ^a	Cl-Si	0.5785 ^a
	—	—		—		0.4235 ^b
	—	—		—		—
	1.8612 ^d	5.5369 ^d		-0.3982 ^d		—
Pt	0.4112 ^a	0.6170 ^a	1.9754 ^a	6.9965 ^a	Pt-Si	—
	0.4387 ^b	0.5974 ^b	1.3024 ^b	7.6616 ^b		—
	0.2372 ^c	0.4920 ^c	1.4661 ^c	7.8045 ^c		0.1092 ^c
	0.6591 ^d	0.8921 ^d	8.5948 ^d	-0.1459 ^d		—
N _I	1.3184 ^a	2.9864 ^a	—	0.6952 ^a	Pt-O	—
	1.3194 ^b	3.4380 ^b	—	0.2426 ^b		—
	1.3573 ^c	3.3924 ^c	—	0.2502 ^c		0.7269 ^c
	1.4273 ^d	2.1555 ^d	—	1.4171 ^d		—
N _{II}	1.4572 ^a	3.3890 ^a	—	0.1537 ^a		
	1.4683 ^b	4.3326 ^b	—	-0.8009 ^b		
	1.3752 ^c	3.6591 ^c	—	-0.0343 ^c		
	1.4586 ^d	2.3163 ^d	—	1.2251 ^d		
Si _I	0.6487 ^a	0.8423 ^a	—	2.5089 ^a		
	0.6490 ^b	0.8736 ^b	—	2.4773 ^b		
	0.7084 ^c	0.8433 ^c	—	2.4483 ^c		
	0.7129 ^d	0.8252 ^d	—	2.4619 ^d		
Si _{II}	0.6690 ^a	0.9295 ^a	—	2.4014 ^a		
	0.7602 ^b	0.8854 ^b	—	2.3544 ^b		
	0.6954 ^c	0.8043 ^c	—	2.5002 ^c		
	0.7557 ^d	0.8537 ^d	—	2.3906 ^d		
Si _{III}	0.5832 ^a	0.9806 ^a	—	2.4362 ^a		
	0.5846 ^b	0.9862 ^b	—	2.4292 ^b		
	0.5885 ^c	0.9482 ^c	—	2.4632 ^c		
	0.5848 ^d	0.9881 ^d	—	2.4271 ^d		
O _I	1.6135 ^a	5.3967 ^a	—	-1.0101 ^a		
	1.6160 ^b	5.4476 ^b	—	-1.0635 ^b		
	1.5993 ^c	5.0873 ^c	—	-0.6866 ^c		
	1.6020 ^d	4.7942 ^d	—	-0.3962 ^d		
O _{II}	1.6678 ^a	5.5382 ^a	—	-1.2059 ^a		
	1.6484 ^b	5.4856 ^b	—	-1.1339 ^b		
	1.6066 ^c	4.8620 ^c	—	-0.4687 ^c		
	1.6473 ^d	5.3482 ^d	—	-0.9955 ^d		

^a *cis*-[PtCl₂(NH₃)₂]/silica-NH₂ system, ^b *cis*-[PtCl(NH₃)₂]⁺/silica-NH₂ system.^c *cis*-[Pt(NH₃)₂]²⁺/silica-NH₂ system, ^d isolated silica-NH₂, or isolated *cis*platin.

changes occur in N *p*, Si (superficial) *s*, and O *p* orbitals. Noticeable changes can be observed in *cis*-platin orbitals. The Cl *s* and Cl *p* populations decrease 17% and 35%, respectively, while Pt *s*, Pt *p* and Pt *d* populations decrease 33%, 33%, and 85%, respectively. For *cis*-[PtCl(NH₃)₂]⁺-silica-NH₂ system, the *s* and *p* orbital populations of the N atoms neighbouring to *cis*-platin decrease to about 5%

and increase 58%, respectively. The *s* and *p* populations of neighbouring Si (superficial) atoms are modified by 1–8% and 2–6%, respectively, while Si (bulk) population changes 1–4%. The *s* and *p* orbital populations of the O atoms neighbouring to *cis*-platin is modified to about 2% and 6–9% respectively. Then, the major population changes occur in N *p* orbitals. Big changes take place in Pt atomic orbitals of *cis*-platin molecule.

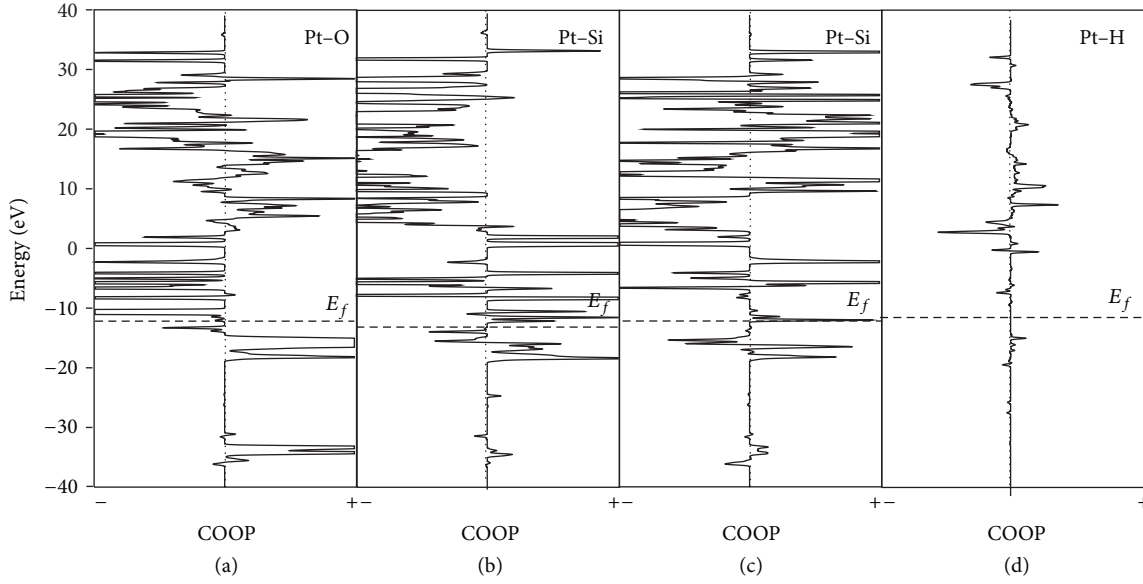


FIGURE 9: COOP curves of (a) Pt-O, (b) Pt-Si, (c) Pt-Si (bulk), and (d) Pt-H interactions for *cis*-[Pt(NH₃)₂]²⁺ adsorption.

TABLE 4: Average overlap population (OP).

Bond	OP
N-Si	0.212 ^a
	0.224 ^b
	0.311 ^c
	0.497 ^d
O-Si (surface)	0.645 ^a
	0.522 ^b
	0.329 ^c
	0.700 ^d
O-Si (bulk)	0.512 ^a
	0.510 ^b
	0.476 ^c
	0.592 ^d
N-H	0.613 ^a
	0.650 ^b
	0.594 ^c
	0.725 ^d
Pt-Cl	0.592 ^a
	0.779 ^b
	—
	0.534 ^d

^a*cis*-[PtCl₂(NH₃)₂]/silica-NH₂ system, ^b*cis*-[PtCl(NH₃)₂]⁺/silica-NH₂ system.

^c*cis*-[Pt(NH₃)₂]²⁺/silica-NH₂ system, ^disolated silica-NH₂, or isolated *cis*platin.

The Pt *s*, Pt *p*, and Pt *d* populations decrease 64%, 45%, and 83%, respectively.

The new interactions are formed at the expenses of the original bonds (see Table 4). When Cl-N and Cl-Si interactions are formed during *cis*-[PtCl₂(NH₃)₂] and *cis*-[PtCl(NH₃)₂]⁺ adsorption, the N-Si and Si-O (superficial)

bond strengths are reduced between 47–55% and 8–24%, respectively, while the Si-O (bulk) interaction increases to about 2 %, compared with the same bonds in the isolated surface. On the other hand, when Pt-O, Pt-Si, and Pt-H interactions are formed during *cis*-[Pt(NH₃)₂]²⁺ adsorption, the N-Si, Si-O (superficial), and N-H bond strengths are modified to about 5–29%, 5–20%, and 4–17%, respectively, after adsorption. At the same time, the Pt-Cl bond of both *cis*-[PtCl₂(NH₃)₂] molecule and the *cis*-[PtCl(NH₃)₂]⁺ complex are strengthened 11% and 46%, respectively, after adsorption.

5. Conclusions

The adsorption of *cis*-platin drug on a SiO₂(100) hydrated surface was investigated by computational calculation. During adsorption, the silica surface maintains its matrix properties and the major changes occur in *cis*-platin's molecule. The *cis*-platin molecule presents weak interactions with neighbouring OH groups of the hydrated surface and the hydrolysis process is not favourable on the SiO₂(100) surface.

The SiO₂(100) adsorption properties are improved considering the surface's modification with K, Mg, or NH₂ chemical species. In general, the stability of the system is increased and the molecule-surface distance is reduced. The hydrolysis is a favourable process on the SiO₂(100) functionalized surface. The adsorption of *cis*-platin molecule and its complexes is strengthened. The electron density exchange between the functional specie and the molecule/complexes plays a main role in the adsorption process. The *cis*-platin hydrolysis is most favoured when the surface is functionalized with the NH₂ specie. *cis*-[PtCl₂(NH₃)₂] and *cis*-[PtCl(NH₃)₂]⁺ are adsorbed on the surface via Cl-N and Cl-Si interactions, while the *cis*-[Pt(NH₃)₂]²⁺ complex is adsorbed through Pt-O, Pt-Si, and Pt-H interactions. After adsorption, the strength of N-Si, Si-O and N-H superficial bond of the

functionalized SiO₂(100) changes favoring the interaction between the molecule and its complexes with the surface.

Acknowledgments

This work was supported by SGCyT UNS, PIP-CONICET, and PICT. G. Brizuela and S. Simonetti are members of CONICET. A. Díaz Compañy is a fellow of Comisión de Investigaciones Científicas (CIC) de la provincia de Buenos Aires.

References

- [1] V. P. Zhdanov, *Elementary Physical-Chemical Processes on Surface*, Nauka, Novosibirsk, Russia, 1988.
- [2] M. Jaroniec and R. Madey, *Physical Adsorption on Heterogeneous Solids*, Elsevier, Amsterdam, The Netherlands, 1988.
- [3] F. Joachim, A. Vidal, and E. Papirer, in *Chemically Modified Oxide Surfaces*, E. Leyden and W. T. Collins, Eds., p. 361, Gordon and Breach, New York, NY, USA, 1990.
- [4] V. M. Ogenko, V. M. Rosenbaum, and A. A. Chuiko, *The Theory of Vibrations and Reorientations of Surface Atomic Groups*, Naukova Dumka, Kiev, Ukraine, 1991.
- [5] A. A. Chuiko and Y. I. Gorlov, *Surface Chemistry of Silica: Surface Structure, Active Sites, Sorption Mechanisms*, Naukova Dumka, Kiev, Ukraine, 1992.
- [6] A. A. Chuiko, Ed., *Silicas in Medicine and Biology*, Institute of Surface Chemistry, National Academy of Science of Ukraine, Kiev, Ukraine, 1993.
- [7] G. A. Somarjai, *Introduction to Surface Chemistry and Catalysis*, John Wiley & Sons, New York, NY, USA, 1994.
- [8] E. F. Vansant, P. van der Voort, and K. C. Vrancken, *Characterization and Chemical Modification of the Silica Surface*, Elsevier, Amsterdam, The Netherlands, 1995.
- [9] A. Dabrowski and V. A. Tertykh, Eds., *Adsorption on New and Modified Inorganic Sorbents*, Elsevier, Amsterdam, The Netherlands, 1996.
- [10] A. P. Legrand, Ed., *The Surface Properties of Silicas*, John Wiley & Sons, London, UK, 1998.
- [11] M. R. Linford and C. E. D. Chidsey, "Surface functionalization of alkyl monolayers by free-radical activation: gas-phase photochlorination with Cl₂," *Langmuir*, vol. 18, no. 16, pp. 6217–6221, 2002.
- [12] A. Juang, O. A. Scherman, R. H. Grubbs, and N. S. Lewis, "Formation of covalently attached polymer overlayers on Si(111) surfaces using ring-opening metathesis polymerization methods," *Langmuir*, vol. 17, no. 5, pp. 1321–1323, 2001.
- [13] L. C. P. M. de Smet, G. A. Stork, G. H. F. Hurenkamp et al., "Covalently attached saccharides on silicon surfaces," *Journal of the American Chemical Society*, vol. 125, no. 46, pp. 13916–13917, 2003.
- [14] T. Böcking, M. James, H. G. L. Coster, T. C. Chilcott, and K. D. Barrow, "Structural characterization of organic multilayers on silicon (111) formed by immobilization of molecular films on functionalized Si–C linked monolayers," *Langmuir*, vol. 20, no. 21, pp. 9227–9235, 2004.
- [15] J. T. C. Wojtyk, K. A. Morin, R. Boukherroub, and D. D. M. Wayner, "Modification of porous silicon surfaces with activated ester monolayers," *Langmuir*, vol. 18, no. 16, pp. 6081–6087, 2002.
- [16] M. Vallet-Regi, A. Rámila, R. P. Del Real, and J. Pérez-Pariente, "A new property of MCM-41: drug delivery system," *Chemistry of Materials*, vol. 13, no. 2, pp. 308–311, 2001.
- [17] J. Zhao, F. Gao, Y. Fu, W. Jin, P. Yang, and D. Zhao, "Biomolecule separation using large pore mesoporous SBA-15 as a substrate in high performance liquid chromatography," *Chemical Communications*, no. 7, pp. 752–753, 2002.
- [18] P. J. O'Dwyer and J. P. Stevenson, "Clinical status of cisplatin, carboplatin, and other platinum-based antitumor drugs," in *Cisplatin*, B. Lippert, Ed., pp. 31–72, Wiley-VCH, Weinheim, Germany, 1999.
- [19] Y. R. Rodríguez and C. H. Castro, "Avances recientes en la determinación analítica del cisplatino y sus productos de hidrólisis," *Revista CENIC. Ciencias Químicas*, vol. 40, no. 1, 2009.
- [20] J. P. Reedijk, "New clues for platinum antitumor chemistry: kinetically controlled metal binding to DNA," *Proceedings of the National Academy of Sciences of the United States of America*, vol. 100, no. 7, pp. 3611–3616, 2003.
- [21] M. A. Jakupiec, M. Galanski, and B. K. Keppler, "Tumour-inhibiting platinum complexes-state of the art and future perspectives," *Reviews of Physiology, Biochemistry and Pharmacology*, vol. 146, pp. 1–53, 2003.
- [22] A. Sigel and H. Sigel, Eds., *Metal Ions in Biological Systems*, vol. 42, Marcel Dekker, New York, NY, USA, 2004.
- [23] D. Wang and S. J. Lippard, "Cellular processing of platinum anticancer drugs," *Nature Reviews Drug Discovery*, vol. 4, no. 4, pp. 307–320, 2005.
- [24] J. V. Burda, M. Zeizinger, and J. Leszczynski, "Hydration process as an activation of trans- and cisplatin complexes in anticancer treatment. DFT and Ab initio computational study of thermodynamic and kinetic parameters," *Journal of Computational Chemistry*, vol. 26, no. 9, pp. 907–914, 2005.
- [25] V. Troger, J. L. Fischel, P. Formento, J. Gioanni, and G. Milano, "Effects of prolonged exposure to cisplatin on cytotoxicity and intracellular drug concentration," *European Journal of Cancer*, vol. 28, no. 1, pp. 82–86, 1992.
- [26] R. B. Weiss and M. C. Christian, "New cisplatin analogues in development: a review," *Drugs*, vol. 46, no. 3, pp. 360–377, 1993.
- [27] A. Uchida, Y. Shinto, N. Araki, and K. Ono, "Slow release of anticancer drugs from porous calcium hydroxyapatite ceramic," *Journal of Orthopaedic Research*, vol. 10, no. 3, pp. 440–445, 1992.
- [28] K. Ajima, T. Murakami, Y. Mizoguchi et al., "Enhancement of in vivo anticancer effects of cisplatin by incorporation inside single-wall carbon nanohorns," *ACS Nano*, vol. 2, no. 10, pp. 2057–2064, 2008.
- [29] S. Simonetti, A. D. Compañy, G. Brizuela, and A. Juan, "Theoretical study of cisplatin adsorption on silica," *Applied Surface Science*, vol. 258, no. 3, pp. 1052–1057, 2011.
- [30] A. D. Compañy, A. Juan, G. Brizuela, and S. Simonetti, "Effect of thiol-functionalised silica on cisplatin adsorption," *Molecular Simulation*, vol. 38, no. 13, pp. 1055–1060, 2012.
- [31] S. Simonetti, A. D. Compañy, G. Brizuela, and A. Juan, "Modeling of CN-functionalized silica as vehicle for delivery of the chemotherapeutic agent: cisplatin," *Applied Physics A*, vol. 109, no. 1, pp. 63–68, 2012.
- [32] G. Landrum and W. Glassey, *Yet Another Extended Hückel Molecular Orbital Package (YAEHMOP)*, Cornell University, Ithaca, NY, USA, 2004.

- [33] J. H. de Boer, *The Structure and Properties of Porous Materials*, edited by D. H. Everett and F. S. Stone, Butterworth, London, UK, 1958.
- [34] G. H. Milburn and M. R. Truter, "The crystal structures of cis- and trans-dichlorodiammineplatinum(II)," *Journal of the Chemical Society A*, pp. 1609–1616, 1966.
- [35] R. Shandles, E. O. Schlemper, and R. K. Murmann, "The crystal and molecular structure of tetraammineplatinum(II) μ -oxo-bis[oxotetracyanorhenium(V)]," *Inorganic Chemistry*, vol. 10, no. 12, pp. 2785–2789, 1971.
- [36] A. Robertazzi and J. A. Platts, "Hydrogen bonding, solvation, and hydrolysis of cisplatin: a theoretical study," *Journal of Computational Chemistry*, vol. 25, no. 8, pp. 1060–1067, 2004.
- [37] R. Hoffmann and W. N. Lipscom, "Theory of polyhedral molecules. I. Physical factorizations of the secular equation," *Journal of Chemical Physics*, vol. 36, no. 8, pp. 2179–2195, 1962.
- [38] R. Hoffmann, "An extended Hückel theory. I. Hydrocarbons," *Journal of Chemical Physics*, vol. 39, no. 6, pp. 1397–1412, 1963.
- [39] M. Whangbo and R. Hoffmann, "The band structure of the tetracyanoplatinate chain," *Journal of the American Chemical Society*, vol. 100, no. 19, pp. 6093–6098, 1978.
- [40] A. Anderson, "Derivation of the extended Hückel method with corrections: one electron molecular orbital theory for energy level and structure determinations," *Journal of Chemical Physics*, vol. 62, no. 3, pp. 1187–1188, 1975.
- [41] A. Anderson and R. Hoffmann, "Description of diatomic molecules using one electron configuration energies with two-body interactions," *Journal of Chemical Physics*, vol. 60, no. 11, pp. 4271–4273, 1974.
- [42] K. Sun, M. Kohyama, S. Tanaka, and S. Takeda, "Theoretical study of atomic oxygen on gold surface by Hückel theory and DFT calculations," *Journal of Physical Chemistry A*, vol. 116, no. 38, pp. 9568–9573, 2012.
- [43] K. Sun, M. Kohyama, S. Tanaka, and S. Takeda, "A theoretical study of CO adsorption on gold by Hückel theory and density functional theory calculations," *Journal of Computational Chemistry*, vol. 32, no. 15, pp. 3276–3282, 2011.
- [44] M. Oana, R. Homann, H. Abruña, and F. DiSalvo, "Adsorption of CO on PtBi₂ and PtBi surfaces," *Surface Science*, vol. 574, no. 1, pp. 1–16, 2005.
- [45] M. B. Fernández, G. M. Tonetto, G. H. Crapiste, M. L. Ferreira, and D. E. Damiani, "Hydrogenation of edible oil over Pd catalysts: a combined theoretical and experimental study," *Journal of Molecular Catalysis A*, vol. 237, no. 1–2, pp. 67–79, 2005.
- [46] S. Simonetti, C. Lanz, and G. Brizuela, "Hydrogen embrittlement of a Fe–Cr–Ni alloy: analysis of the physical and chemical processes in the early stage of stress corrosion cracking initiation," *Solid State Sciences*, vol. 15, pp. 137–141, 2013.
- [47] S. Simonetti, S. Ulacco, G. Brizuela, and A. Juan, "Computational study of cis-oleic acid adsorption on Ni(111) surface," *Applied Surface Science*, vol. 258, no. 15, pp. 5903–5908, 2012.

